JACS
JOURNAL OF THE AMERICAN CHEMICAL SOCIETY
Communication
pubs.acs.org/JACS

Water Durable Electride Y_5Si_3: Electronic Structure and Catalytic Activity for Ammonia Synthesis

Yangfan Lu,[†,‡,#] Jiang Li,[†,‡,#] Tomofumi Tada,[†] Yoshitake Toda,[†,‡] Shigenori Ueda,[§,∥] Toshiharu Yokoyama,[†,‡] Masaaki Kitano,[†] and Hideo Hosono*[,†,‡]

[†]Materials Research Center for Element Strategy, Tokyo Institute of Technology, 4259 Nagatsuta, Midori-ku, Yokohama 226-8503, Japan

[‡]ACCEL, Japan Science and Technology Agency, 4-1-8 Honcho, Kawaguchi, Saitama 332-0012, Japan

[§]Synchrotron X-ray Station at SPring-8, National Institute for Material Science (NIMS), 1-1-1 Kouto, Sayo, Hyogo 679-5148, Japan

[∥]Quantum Beam Unit, NIMS, 1-2-1 Sengen, Tsukuba 305-0047, Japan

Supporting Information

ABSTRACT: We report an air and water stable electride Y_5Si_3 and its catalytic activity for direct ammonia synthesis. It crystallizes in the Mn_5Si_3-type structure and confines 0.79/f.u. anionic electrons in the quasi-one-dimensional holes. These anionic electrons strongly hybridize with yttrium 4d electrons, giving rise to improved chemical stability. The ammonia synthesis rate using Ru(7.8 wt %)-loaded Y_5Si_3 was as high as 1.9 mmol/g/h under 0.1 MPa and at 400 °C with activation energy of ∼50 kJ/mol. Its strong electron-donating ability to Ru metal of Y_5Si_3 is considered to enhance nitrogen dissociation and reduce the activation energy of ammonia synthesis reaction. Catalytic activity was not suppressed even after Y_5Si_3, once dipped into water, was used as the catalyst promoter. These findings provide novel insights into the design of simple catalysts for ammonia synthesis.

Electrides are the materials that accommodate a finite anionic electron density which does not belong to any particular orbitals.[1,2] The presence of anionic electrons was first proposed in the alkali metal-sandwiched crown ether, $A^+(18C_6)_2{:}e^-$ (A = alkali metals), and have attracted much attention due to its exotic natures.[3,4] The organic electrides, however, are not suitable for practical applications since they are highly sensitive to air, water, and even thermal energy. To improve chemical stability of electrides, it has been attempted to isolate anionic electrons in an inorganic lattice. In 2003, Matsuishi et al. reported that 2×10^{21} cm^{-3} of anionic electron density can be isolated in the cage-like lattice of $[Ca_{24}Al_{28}O_{64}]^{4+}(e^-)_4$ (C12A7:e^-) by removing free oxygen ions of the parent compound $[Ca_{24}Al_{28}O_{64}]^{4+}(O^{2-})_2$.[5] The anionic electrons confined in C12A7:e^- give rise to an interstitial band at the Fermi level and reduce the work function to be 2.4 eV.[5,6] After the discovery of C12A7:e^-, Ca_2N and Y_2C appeared as new inorganic electrides, however, none of them are stable in water.[7,8]

One of the successful applications of inorganic electrides is the direct ammonia synthesis which requires both high-pressure and -temperature conditions in the Haber−Bosch process.[9] The primary difficulty and the rate-limiting step in the traditional process is the dissociation of nitrogen molecules, known as the strongest chemical bonding among diatomic molecules.[9,10] Recently, Kitano et al. demonstrated that ruthenium (Ru)-loaded C12A7:e^- (Ru/C12A7:e^-) shows excellent catalytic activity for ammonia synthesis even under an ambient pressure.[11] It was discussed that highly activated electrons inherent in C12A7:e^- encourage nitrogen dissociation on Ru surface and reduce the activation energy (E_a) of ammonia synthesis.[12] However, since Ru/C12A7:e^- degrades catalytic activity once water is absorbed, the catalyst cannot be applied to chemical reactions including liquid processes. It is therefore in high demand to explore new water stable electrides for ameliorating general versatility of the catalysts.

Herein we report that Y_5Si_3 is the first discovered water stable electride, and Ru-loaded Y_5Si_3 (Ru/Y_5Si_3) is highly efficient for direct ammonia synthesis. Y_5Si_3 was revealed to be a new class of electrides which exhibits strong orbital hybridization between yttrium 4d and anionic electrons. The obtained experimental data are consistent with the theoretical calculations which indicate that Y_5Si_3 is an electride with a formula of $[Y_5Si_3]^{0.79+}{:}0.79e^-$. We will show the turnover frequency (TOF) and E_a of ammonia synthesis were improved by Ru/Y_5Si_3 and discuss the anionic electrons confined in Y_5Si_3 as a possible key ingredient for encouraging nitrogen dissociation.

Polycrystalline Y_5Si_3 samples were synthesized using the arc-melting method as reported previously (dry Y_5Si_3).[13] The wet Y_5Si_3 samples were prepared by exposing dry Y_5Si_3 into distilled water for 1 h. The powder X-ray diffraction (XRD) patterns were taken using a Bruker D8 Advance diffractometer with Cu Kα radiation at room temperature. Transport, magnetic, and thermodynamic properties of Y_5Si_3 were measured using PPMS and SVSM (Quantum Design). Photoelectron spectroscopy measurements were performed with both the undulator beamline BL15XU of SPring-8 (HAXPES, $h\nu$ = 5953.4 eV) and a He I discharge lamp light source (UPS, $h\nu$ = 21.2 eV) at room temperature.[14,15] Density functional theory calculations were performed using the generalized gradient approximation with the Perdew−Burke−Ernzerhof functional and the

Received: January 6, 2016
Published: March 13, 2016

DOI: 10.1021/jacs.6b00124
J. Am. Chem. Soc. 2016, 138, 3970−3973

projector augmented plane wave method implemented in the Vienna ab initio simulation program (VASP 5.2).[16,17] Ammonia syntheses were conducted in silica and stainless tubes with Ru/Y_5Si_3. The produced ammonia was trapped in a 5 mM sulfuric acid solution, and the amount of NH^{4+} generated in the solution was determined using ion chromatography with a conductivity detector (Prominence, Shimadzu).[11,12]

Figure 1a shows the crystal structure of Y_5Si_3.[13,18] It crystallizes in the Mn_5Si_3-type structure ($P6_3/mcm$) and has

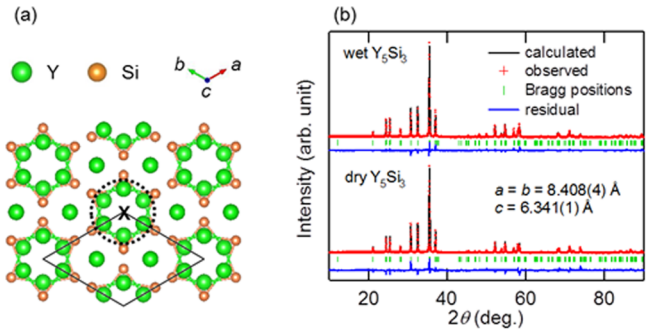

Figure 1. (a) The crystal structure of Y_5Si_3. Yttrium and silicon atoms are depicted using green and orange balls. (b) Powder XRD patterns for dry and wet Y_5Si_3. Reliability parameters are R_{wp} = 5.640%, R_e = 2.650% for dry and R_{wp} = 7.154%, R_e = 4.020% for wet samples, respectively.

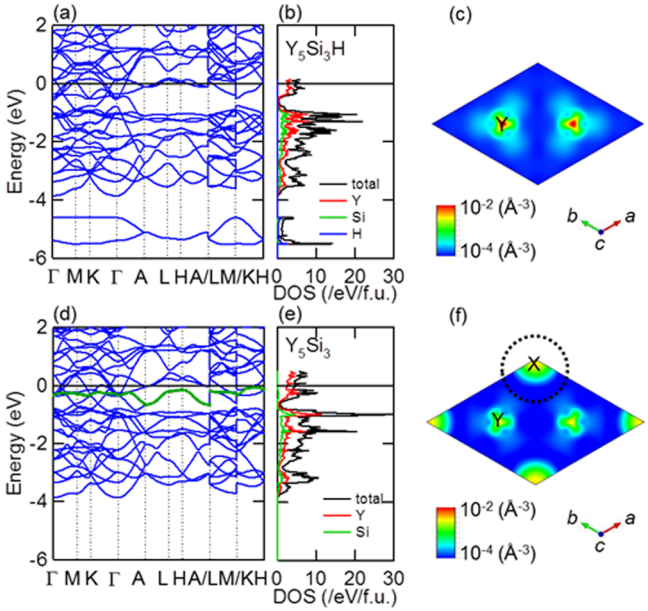

Figure 2. (a) Electronic band structure, (b) DOSs, and (c) electron density map for the (001) plane of Y_5Si_3H. Electronic structures for Y_5Si_3 are represented in (d–f) as well as Y_5Si_3H. The interstitial contribution is emphasized using the green line. Electron density map of both Y_5Si_3H and Y_5Si_3 was calculated using the energy range of −0.5 eV < $E - E_F$ < 0.0 eV.

been studied as a hydrogen storage material.[19] One of the highlighted characters of the material is occurrence of the quasi-one-dimensional (1D) holes along the *c*-axis as emphasized by the black dashed circle. The diameter of the hole is as long as ∼4 Å, and it was reported that the interstitial site, denoted as X, can accommodate hydrogens, forming Y_5Si_3H.[19] The powder XRD pattern in the lower panel of Figure 1b shows that the obtained dry Y_5Si_3 is a single phase, and the refined lattice parameters are in good agreement with the previous study.[13,20] No decomposition can be noted for wet Y_5Si_3, revealing durability against water (the upper panel of Figure 1b).

The band structure, electronic density of states (DOS), and electron density map of both Y_5Si_3H and Y_5Si_3 are shown in Figure 2. We first consider the electronic structure of Y_5Si_3H since it can be regarded as a parent compound of Y_5Si_3. The Fermi level of Y_5Si_3H is partially composed of yttrium 4d orbitals, while the hydrogen 1s orbital is located at ∼5 eV below the Fermi level, giving the formal valence state to be $[Y_5Si_3]^+(H^-)$. In this case, the interstitial site is occupied by H^- ion, and no free electron density is expected in the quasi-1D holes (Figure 2a–c). In hydrogen-free Y_5Si_3, the yttrium 4d orbitals contribute to the Fermi level as well as Y_5Si_3H, while an extra band emerges just below the Fermi level (Figure 2d,e). Since removing a H^- ion can be regarded as electron doping, the electrons are suggested to be confined in the yttrium 4d orbitals within the rigid band model.[21] However, appearance of the extra band strongly implies that the electrons are not confined in any particular orbitals, but interstitial site X (Figure 2f). Indeed, the calculation revealed that 0.96/f.u. electrons increase by removing H^- ion, while only 0.17/f.u. electrons do for the Y_5Si_3 lattice in the energy range of −4 eV < $E - E_F$ < 0 eV. This result implies that the rest of electrons behave as anions, and therefore the chemical formula can be described as $[Y_5Si_3]^{0.79+}$:0.79e^-. The theoretically expected electronic structure is consistent with the picture of electrides as discussed previously.[5,6]

Y_5Si_3 exhibits metallic conductivity with the electronic resistivity of ρ = 1.26 × 10^{-4} Ω·cm at 300 K (Figure 3a). The $\rho(T)$ decreases with lowering temperature and can be fitted by the formula $\rho(T) = \rho(0) + AT^n$, where n is 3.61 in the temperature range of 2 K < T < 20 K. The n value obtained is larger than 2 and smaller than the conventional Bloch–Gruneisen formula (n = 5), implying that interband electron–phonon scattering dominates the electron scattering process in Y_5Si_3 below 20 K. Such a complicated electron scattering process attributes to the multiple bands nature of Y_5Si_3. The magnetoresistance (MR) also suggests the presence of multiple Fermi surfaces in Y_5Si_3 (the inset of Figure 3a). The observed MR is nonquadratic at high fields and low temperatures. Furthermore, the magnitude of MR at 2 K is ∼10% which is one order larger than that of the conventional single carrier metals, such as copper, implying the presence of multiple carriers with different mobilities.[22]

The magnetic susceptibility χ of Y_5Si_3 shows a nonmagnetic behavior and is almost temperature independent (Figure 3b). Since Pauli paramagnetism as well as Sommerfeld constant γ directly reflect the DOS at the Fermi level ($D(\varepsilon_F)$), we could check the consistency with the theoretical calculations. The magnitude of χ at 0 K is estimated to be $\chi(0)$ = 1.82 × 10^{-4} emu/mol by extrapolating from the high-temperature region. The γ is obtained using conventional Debye model, $C/T = \gamma + \beta T^2$, giving γ = 12.9 mJ/(mol K^2) and β = 0.767 mJ/(mol K^4), respectively (the inset of Figure 3b). With combination of $\chi(0)$ and γ, we could calculate the Wilson ratio to be $R_w = \pi^2 k_B^2 \chi(0)/(3\ \mu_B^2 \gamma) \sim 1$ which is identical to the free electron value. Here k_B and μ_B are the Boltzmann constant and Bohr magneton, respectively. The magnitude of γ is in good agreement with the theoretical expectation which estimates

DOI: 10.1021/jacs.6b00124
J. Am. Chem. Soc. 2016, 138, 3970–3973

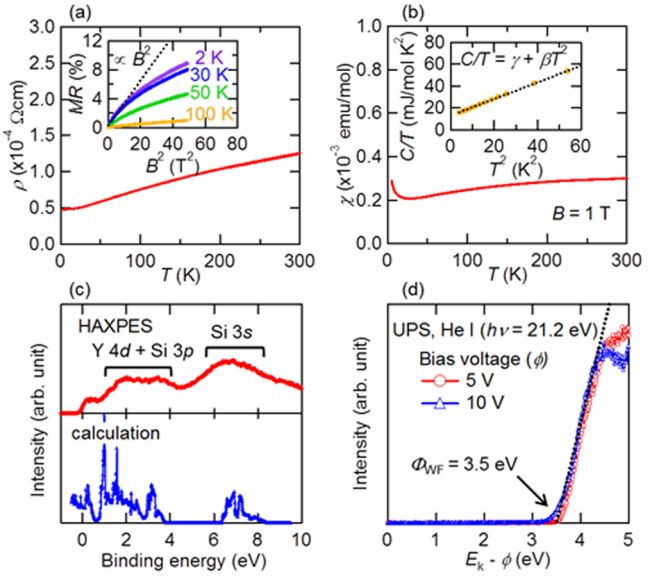

Figure 3. (a) Resistivity of Y_5Si_3 as a function of temperature. Inset shows magnetoresistance as a function of B^2. The black dashed line represents quadratic field dependence. (b) Magnetic susceptibility of Y_5Si_3 measured under B = 1 T. Inset shows the specific heat divided by temperature as a function of T^2. The black dashed line represents conventional Debye fitting. (c) Valence band HAXPES spectrum (upper panel) and calculated total DOS of Y_5Si_3 (lower panel). Energy of incident X-rays used was 5953.4 eV, and escape depth of photoelectron is on the order of ~10 nm. (d) Secondary electron cutoff of the Y_5Si_3 polycrystalline sample measured using UPS with different bias voltages (ϕ = 5 and 10 V).

the DOS to be $D(\varepsilon_F)$ = 5.07 states/eV/f.u., giving $\gamma^{cal} = \pi^2 k_B^2 D(\varepsilon_F)/3$ = 12.0 mJ/(mol K^2).

In order to further confirm the bulk electronic structure of Y_5Si_3, we conducted a hard X-ray photoemission spectrum (HAXPES) which is bulk sensitive (Figure 3c).[14,15] A clear Fermi edge can be identified, revealing metallic nature in Y_5Si_3. The HAXPES spectrum shows three weak peaks at 1.8, 3.5, and 6.7 eV, consistent with the calculated total DOS features in terms of bandwidths and positions. The obtained valence band spectrum is less variety of structure compared to Y_2C due to extended silicon 3p orbitals.[8] The work function (Φ_{WF}) of Y_5Si_3 was determined from the cutoff of the secondary electron measured by UPS (Figure 3d). The Φ_{WF} estimated is ~3.5 eV and lower than the other transition-metal silicides, reflecting the loosely bound nature of anionic electrons in Y_5Si_3. The obtained work function is slightly higher than the previously studied electrides since the chemical potential of anionic electron might be stabilized through strong interaction with the yttrium 4d electrons in Y_5Si_3.[6−8]

The experimentally obtained data are consistent with the theoretical calculations revealing that Y_5Si_3 is an electride with 0.79/f.u anionic electrons. It is noteworthy that these anionic electrons strongly hybridize with yttrium 4d orbitals. As a consequence, bandwidths of the yttrium 4d orbitals are enlarged compared to Y_5Si_3H, i.e., non-electride case (Figure 2d). The tendency cannot be interpreted within a chemical pressure effect since the unit cell volume of Y_5Si_3H is smaller than that of Y_5Si_3. Such orbital hybridization is in contrast to the previously studied electrides, including C12A7:e$^-$ and Ca_2N.[5,6,20] In these electrides, anionic electrons are spatially separated, and DOS at the Fermi level is dominated by anionic electron bands. We argue that a water stable electride is realized in Y_5Si_3 since the orbital hybridization gives rise to a chemical bond formation which stabilizes and protects the anionic electrons from unintended chemical reactions.

The coexistence of highly activated electrons and improved chemical stability allows us to challenge the direct ammonia synthesis using Y_5Si_3 as a catalyst promoter. Figure 4a shows

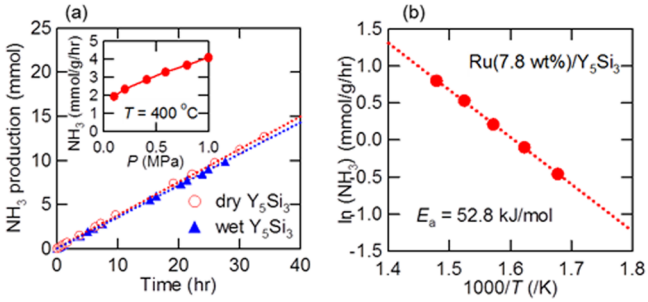

Figure 4. (a) Ammonia production using Ru(7.8 wt %)/Y_5Si_3 as catalyst under an ambient pressure (0.1 MPa). 0.2 g of catalyst was used, and H_2/N_2 = 3 mixed gas was reacted at 400 °C with a flow rate of 60 mL/min. Dry and wet Y_5Si_3 powders were used as catalyst promoter, respectively. Inset represents the ammonia production rate as a function of synthetic pressure. (b) The Arrhenius plot of ammonia production in the temperature range of 320 °C − 400 °C.

the catalytic activity of Ru(7.8 wt %)/Y_5Si_3 for ammonia synthesis as a function of time under an ambient pressure. The catalyst continuously produced ammonia (1.9 mmol/g/h) without decreasing catalytic activity for 36 h. The ammonia synthesis rate was furthermore enhanced with increasing total synthetic pressure and reached 4.1 mmol/g/h under 1.0 MPa and at 400 °C (inset of Figure 4a). The synthesis rate obtained is comparable to the well-studied ammonia synthesis catalysts, such as Ru−Cs/MgO and Ru−Ba/activated carbon (AC), despite a much lower dispersion and surface area as summarized in Table S1.[11,23,24] Remarkably, Y_5Si_3 was found to be robust against water. We conducted ammonia synthesis using wet Y_5Si_3 powder as catalyst promoter without changing any other conditions. The obtained ammonia synthesis rate is almost identical to that of dried catalyst (Figure 4a). In addition, the catalyst exhibited a stable cycle property and did not degrade even when ~3% of vapor pressure of water was introduced into the reactor for 1 h between each run, evidencing durability of Y_5Si_3 against water (Figure S1).

The excellent catalytic activity of Ru/Y_5Si_3 for ammonia synthesis is attributed to its high TOF and low E_a. The TOF for Ru(7.8 wt %)/Y_5Si_3 was as high as 0.067 s^{-1} (400 °C, 0.1 MPa), which was several times higher than the other Ru-loaded catalysts including Cs−Ru/MgO and Ba−Ru/AC.[11,23,24] The E_a of Ru/Y_5Si_3, on the other hand, was estimated to be ~50 kJ/mol from the Arrhenius plot (Figure 4b). The E_a obtained is much smaller than the well-studied catalysts (~100 kJ/mol) while very close to that of Ru/C12A7:e$^-$, suggesting similarities in the reaction mechanism.[11,12] Due to the metallic and low work function natures of Y_5Si_3 (Φ_{WF} = 3.5 eV), the free electrons can be efficiently donated from Y_5Si_3 to Ru metal (Φ_{WF} = 4.7 eV).[25,26] As a consequence, highly activated electrons are transferred into the antibonding π^*-orbitals (LUMO) of nitrogen molecules on Ru surface and significantly weaken its chemical bonding. Nitrogen dissociation is therefore no longer the rate-limiting step, while formation of N−H$_x$ species is considered to dominate the ammonia synthesis

DOI: 10.1021/jacs.6b00124
J. Am. Chem. Soc. 2016, 138, 3970−3973

reaction. It was discussed in Ru/C12A7:e^- that the energy difference between the top of potential barrier for N−H_x formation and reactant molecules, calculated to be ∼50 kJ/mol, corresponds to the E_a of the ammonia synthesis reaction.[12] This value is in good agreement with the case of Ru/Y_5Si_3, and we argue that excellent catalytic activity is realized in Ru/Y_5Si_3 since the activation energy for nitrogen dissociation is significantly reduced. No decomposition of the catalyst can be observed from powder XRD after the ammonia synthesis process (Figure S2). Although Y_5Si_3 absorbs hydrogens as H^- ion during ammonia production, the catalytic activity was not suppressed due plausibly to the reversible hydrogen absorption/desorption ability.[19] The hydrogens incorporated into the Y_5Si_3 are able to react with nitrogen species on the Ru surface, resulting in contiguous ammonia production under both ambient and high-pressure conditions, as discussed in Ru/C12A7:e^-.[11,12]

In summary, Y_5Si_3 was discovered to be the first silicide-related electride stable in both air and water. The present experimental and theoretical studies revealed that Y_5Si_3 confines a finite anionic electron density in the quasi-1D holes which can be described as $[Y_5Si_3]^{0.79+}$:0.79e^-. As distinct from the previously studied electrides, the anionic electrons strongly hybridize with the yttrium 4d electrons, and this effect is considered to improve chemical stability of Y_5Si_3. It was also realized that Ru-loaded Y_5Si_3 could be a promising ammonia synthesis catalyst. The TOF and E_a are much more improved than the well-studied catalysts under both ambient and high-pressure conditions without any additives. Since Y_5Si_3 was synthesized using an one-step method, Ru/Y_5Si_3 can simplify the whole ammonia synthesis process with a combination of chemical stability against both air and water.

■ ASSOCIATED CONTENT

Supporting Information

The Supporting Information is available free of charge on the ACS Publications website at DOI: 10.1021/jacs.6b00124.

Experimental details and data (PDF)

■ AUTHOR INFORMATION

Corresponding Author

*hosono@msl.titech.ac.jp

Author Contributions

#Y.L. and J.L. contributed equally.

Notes

The authors declare no competing financial interest.

■ ACKNOWLEDGMENTS

This work was supported by MEXT Element Strategy Initiative and ACCEL of Japan Science and Technology Agency in Japan. HAXPES measurements were performed with approval of NIMS Synchrotron X-ray Station (proposal nos. 2015A4703 and 2015B4703). S.U. is grateful to HiSOR (Hiroshima University) and JAEA/SPring-8 for the development of HAXPES at BL15XU of SPring-8.

■ REFERENCES

(1) Dye, J. L. *Acc. Chem. Res.* **2009**, *42*, 1564.
(2) Dye, J. L. *Science* **2003**, *301*, 607.
(3) Ellaboudy, A.; Dye, J. L.; Smith, P. B. *J. Am. Chem. Soc.* **1983**, *105*, 6490.
(4) Dale, S. G.; Otero-de-la-Roza, A.; Johnson, E. R. *Phys. Chem. Chem. Phys.* **2014**, *16*, 14584.
(5) Matsuishi, S.; Toda, Y.; Masashi, M.; Katsuro, H.; Toshio, K.; Hirano, M.; Tanaka, I.; Hosono, H. *Science* **2003**, *301*, 626.
(6) Toda, Y.; Yanagi, H.; Ikenaga, E.; Kim, J. J.; Kobata, M.; Ueda, S.; Kamiya, T.; Hirano, M.; Kobayashi, K.; Hosono, H. *Adv. Mater.* **2007**, *19*, 3564.
(7) Lee, K.; Kim, S. W.; Toda, Y.; Matsuishi, S.; Hosono, H. *Nature* **2013**, *494*, 336.
(8) Zhang, X.; Xiao, Z.; Lei, H.; Toda, Y.; Matsuishi, S.; Kamiya, T.; Ueda, S.; Hosono, H. *Chem. Mater.* **2014**, *26*, 6638.
(9) Ertl, G. *Angew. Chem., Int. Ed. Engl.* **1990**, *29*, 1219.
(10) Gambarotta, S.; Scott, J. *Angew. Chem., Int. Ed.* **2004**, *43*, 5298.
(11) Kitano, M.; Inoue, Y.; Yamazaki, Y.; Hayashi, F.; Kanbara, S.; Matsuishi, S.; Yokoyama, T.; Kim, S. W.; Hara, M.; Hosono, H. *Nat. Chem.* **2012**, *4*, 934.
(12) Kitano, M.; Kanbara, S.; Inoue, Y.; Kuganathan, N.; Sushko, P. V.; Yokoyama, T.; Hara, M.; Hosono, H. *Nat. Commun.* **2015**, *6*, 6731.
(13) Parthe, E. *Acta Crystallogr.* **1960**, *13*, 868.
(14) Ueda, S.; Katsuya, Y.; Tanaka, M.; Yoshikawa, H.; Yamashita, Y.; Ishimaru, S.; Matsushita, Y.; Kobayashi, K. *AIP Conf. Proc.* **2009**, *1234*, 403.
(15) Ueda, S. J. *J. Electron Spectrosc. Relat. Phenom.* **2013**, *190*, 235.
(16) Perdew, J. P.; Burke, K.; Ernzerhof, M. *Phys. Rev. Lett.* **1996**, *77*, 3865.
(17) Kresse, G.; Furthmüller, J. *Phys. Rev. B: Condens. Matter Mater. Phys.* **1996**, *54*, 11169.
(18) Momma, K.; Izumi, F. *J. Appl. Crystallogr.* **2011**, *44*, 1272.
(19) McColm, I. J.; Kotroczo, V.; Button, T. W.; Clark, N. J.; Bruer, B. *J. Less-Common Met.* **1986**, *115*, 113.
(20) Izumi, F.; Momma, K. *Solid State Phenom.* **2007**, *130*, 15.
(21) Stern, E. A. *Phys. Rev.* **1967**, *157*, 544.
(22) de Launey, J.; Dolecek, R. L.; Webber, R. T. *J. Phys. Chem. Solids* **1959**, *11*, 37.
(23) Rosowski, F.; Hornung, A.; Hinrichsen, O.; Herein, D.; Muhler, M.; Ertl, G. *Appl. Catal., A* **1997**, *151*, 443.
(24) Liang, C.; Wei, Z.; Xin, Q.; Li, C. *Appl. Catal., A* **2001**, *208*, 193.
(25) Michaelson, H. B. *J. Appl. Phys.* **1977**, *48*, 4729.
(26) Kanbara, S.; Kitano, M.; Inoue, Y.; Yokoyama, T.; Hara, M.; Hosono, H. *J. Am. Chem. Soc.* **2015**, *137*, 14517.

DOI: 10.1021/jacs.6b00124
J. Am. Chem. Soc. 2016, 138, 3970−3973